Fatigue Life Assessment for Welded Structures without Initial Defects: An Algorism for Predicting Fatigue Crack Growth from a Sound Site

Toyosada, Masahiro
Department of Marine Systems Engineering, Kyushu University

Gotoh, Koji
Department of Marine Systems Engineering, Kyushu University

Niwa, Toshio
National Maritime Research Institute Japan, Materials Reliability Group

出版情報：International Journal of Fatigue. 26 (9), pp.993-1002, 2004-09. Elsevier
バージョン：
権利関係：

Fatigue Life Assessment for Welded Structures without Initial Defects: An Algorism for Predicting Fatigue Crack Growth from a Sound Site

Masahiro Toyosada [a,*] , Koji Gotoh [a] and Toshio Niwa [b]

[a] *Kyushu University, Department of Marine Systems Engineering, 6-10-1, Hakozaki, Higashi-ku, Fukuoka, 812-8581, Japan*

[b] *National Maritime Research Institute Japan, Materials Reliability Group, 6-38-1, Shinkawa, Mitaka, Tokyo, 181-0004, Japan*

Abstract

A new fatigue life evaluation methodology, which enables to predict fatigue crack growth from a stress concentration site without the initial defect is proposed. This method is based on the following scenario of fatigue crack growth: (i) a shear mode crack initiates and grows from the stress concentration site, (ii) a crack opening mode appears when the shear crack reaches the first grain boundary, (iii) the crack mode shifts from shear to opening/closing, (iv) opening/closing mode crack propagates. It is further assumed that cracked bodies which have the same stress intensity factor range (ΔK) show the same fatigue crack growth. On the basis of this hypothesis, an equivalent distributed stress (EDS) is defined. EDS corresponds to the distributed stress in an infinite plane with a straight crack for which the relationship between the crack length and the stress intensity factor (K) is the same as

in the considered cracked body. Estimation of fatigue crack growth from a sound stress concentration site in corner boxing joints is performed by applying a fatigue crack closure simulation code FLARP developed by the authors and using the EDS concept. The stresses due to the external loading and welding are converted into EDS in order to apply FLARP.The estimation procedure is validated by comparing the predicted and experimental resutls.

Key words: Fatigue crack mode transition, Micro fracture mechanics, Cyclic Plasticity, Equivalent distributed stress (EDS), FLARP

1 Outline of the fatigue crack opening/closing simulation method for surface cracks

We have developed a fatigue crack opening/closing simulation model for a through thickness crack under an arbitrary stress distribution [1]. Fatigue cracks are generally initiated as plural surface cracks from sound stress concentration sites in an early stage of their life. No cohesive force model for a single surface crack has been proposed yet, because a contour of the fictitious surface crack cannot be described analytically. The basic features of the proposed approximate crack opening/closing simulation in which the plural surface cracks are replaced by a single surface crack are listed below.

(1) A Paris' type crack propagation law, $da/dN = C(\Delta K)^m$, holds for a constant amplitude loading after the steady state closure behaviour de-

* Tel.:+81-92-642-3713
Email address: toyosada@nams.kyushu-u.ac.jp (Masahiro Toyosada).
URL: http://www.nams.kyushu-u.ac.jp/common/production/index_e.html (Masahiro Toyosada).

velops.

(2) It is expected that crack growth curves are almost the same for cracked bodies having the same relationship between the crack length and ΔK.

(3) A reasonable fatigue crack growth curve in terms of the maximum crack depth of a surface crack against the number of cycles can be obtained for plural surface cracks by our procedure. This curve will be considered as the representative crack growth curve.

(4) A procedure to evaluate the influence of neighboring surface cracks on the stress intensity factor at the deepest point of a surface crack is explained in the Appendix.

(5) Stress distribution along a through thickness crack which results in the same change of the stress intenisty factor with the crack depth as for the representative surface crack is found in case of both the applied stresses and the residual stresses. The crack closure analysis for the above mentioned through thickness crack is performed using the model by Toyosada and Niwa [3].

2 Fatigue crack initiation and growth from the root of a notch

For sound (no defect) material at the notch root, slip bands generate first in the planes of a very high atomic density for which the normal vector is nearly perpendicular to the maximum shear stress plane. Because each grain in a polycrystalline material has a different orientation, the slip line has ankles as shown in Fig.1. In Fig.1, the meaning of the symbols are listed below.

θ: the intersection angle of the slip lines in the adjacent grains,

b_i: the intersection points between the slip lines and the boundary of grains,

c: the crack tip at the current loading.

Dislocations move along a slip line and the corresponding normal stresses perpendicular to the slip line are negligible. Although the load which is generated by the existence of the dislocations in other grains ahead of the first grain induces the crack opening, the crack remains closed because of the insufficient density of dislocations and the large distance from the crack tip to the first grain boundary when the crack tip is situated in the middle of the first grain on the notch surface. However, the closer the tip of the shear crack approaches the first grain boundary, the larger the force to open the crack. The large density of dislocations near the crack tip, which moves along the line inclined to the shear crack line due to having a different orientation compared to the slip in the first grain, generates the crack opening force.

It can be assumed that opening mode of crack growth starts when the shear crack reaches the first grain boundary. Research conducted by Forsyth [4] and Gudjact et al. [5] strongly support the above mentioned assumption. Let $\tilde{\omega}$ be the size of overlapping region of the tensile plastic zone at the maximum load (P_{max}) and the compressive plastic zone at the minimum load (P_{min}) in a given loading cycle. It can be presumed that the tip of $\tilde{\omega}$ stays in the initial position until the crack reaches the first grain boundary if a constant amplitude loading is applied, because no opening mode appears and no stress re-distribution takes place. With the proposed approach, the controlling parameter for fatigue crack growth is ΔK_{RPG} [6] throughout the fatigue life

(from the fatigue crack initiation to the failure).The relashionship between $\tilde{\omega}$ and ΔK_{RPG} was formulated as follows by using the numerical fatigue crack growth simulation code by the authors [12].

$$\tilde{\omega} = \eta(\pi/8)(\Delta K_{RPG}/2\lambda\sigma_Y)^2 \tag{1}$$

η in Eq.(1) is a constant and its value is equal to 1.55.

The equivalent ΔK_{RPG} ($(\Delta K_{RPG})_{eq}$)in case of crack propagation in the first grain is obtained from the relationship between ΔK_{RPG} and $\tilde{\omega}$ shown in Eq.(1), see Fig.2 [3].

$$(\Delta K_{RPG})_{eq} = 2\lambda\sigma_Y\sqrt{8\tilde{\omega}/\eta\pi}, \tag{2}$$

where

$$\begin{aligned}
&\tilde{\omega} = r_0 + \tilde{\omega}_s - a, \\
&\tilde{\omega}_s = (\eta\pi/8)(\tilde{U}_s\Delta K_s/2\lambda\sigma_Y)^2, \\
&\tilde{U}_s = (P_{max} - P_{RPG})/(P_{max} - P_{min}) = 1 - 2\lambda\sigma_Y/(P_{max} - P_{min})\sigma_{y0},
\end{aligned}$$

ΔK_s: stress intensity factor range at the deepest point when the surface crack reaches the first grain boundary (semi-circular surface crack is presumed in this case),

$\tilde{\omega}_s$: the size of overlapping region of the tensile plastic zone at the maximum load and the compressive plastic zone at the minimum load when the shear crack reaches the first grain boundary,

r_0: length of the first grain to projected on main crack path,

σ_{y0}: stress at the notch root perpendicular to the main crack when the unit load is applied,

λ: plastic constraint factor (1.04 in the case of mild steel [2]).

It is considered that dislocations can easily move until they reach the first grain boundary. It is presumed that shear crack remains closed during the cyclic loading until a shear crack reaches the first grain boundary. Because not only negative stresses but also positive stresses act on the closed shear crack, the cohesive force model shown in Fig.3 holds at P_{max}. The position of the the fictitious crack tip is obtained based on the assumption that the stress intensity factor for the fictitious crack equals zero. COD at the maximum load for the crack length equal to r_0 can be calculated using the fatigue crack closure simulation model developed by the authors [3]. The length of bar elements in the crack region for both the physical crack and for the fictitious crack at P_{max} can also be computed using the simulation model based on the Dugdale model, because the BCS model [7] provides the same COD profile and the tip of plastic region if the Dugdale model, which the value of shear stress is

substituted into the term of normal stress and the value of shear yield stress is replaced with the tensile yield stress, is applied.

Before the crack reaches the first grain boundary, a cyclic strain, which is almost totally plastic, is generated in every loading cycle near the elastic plastic boundary. Stress keeps the same distribution during the loading because no crack opening occurs in the case of the shear crack and then the elastic plastic boundary does not move under constant amplitude loading. Then the boundary is dominated by the cyclic yield strength (which might be equal to the proportional limit). During the transition stage from a shear crack to an opening/closing crack, yield strength would increase and approach the static yield strength as the crack advances. Yield strength increases as the tip of the tensile plastic zone at maximum load keeps the previous position because of the previous dislocations movement near the elastic plastic boundary at the maximum load. Then it is expected that fatigue crack propagation rate decreases when the crack tip penetrates the first several grains. This phenomenon is in a good agreement with microstructural fracture mechanics [8][9]. Moreover it is expected from this increase of yield strength that the coaxing effect will appear. In other words, a specimen with a sharp notch which has experienced a large amount of cycles at the fatigue limit amplitude can usually have non-propagating cracks. In this case, a small increment of loading amplitude does not lead to growth of the tensile plastic zone over the previous one because of the increase in yield strength during the transition area from shear mode to opening mode of crack growth. It is considered that a compressive plastic zone at the minimum load could not be generated and then the coaxing effect will appear.

3 An example of comparison between the experimental and the estimated life using specimens with a gusset

A numerical simulation code for fatigue crack growth from a sound stress concentration part which accounts for the factors mentioned in the previous chapter and is named "FLARP; Fatigue Life Assessment by RPG load" [3] is developed. By applying FLARP, the fatigue crack growth curve from a stress concentration site without the initial defect can be estimated. Figure 4 is the flowchart of the fatigue crack growth evaluation by using FLARP. (The meaning of the reference crack length is explained later on.) An example of the fatigue crack growth estimation followed by Fig.4 is introduced in this section. Detailed operations of each step in Fig.4 are discussed by using the example from the following problem.

Figure 5 shows a specimen with the gusset, where the fillet weld was done with heat input of 12kJ/cm. The average grain diameter near the weld toe of the steel used is 35μm by the optical observation.

Figure 6 shows the results on the aspect ratio of each surface crack emanating at the boxing fillet weld toe measured by means of the ink penetration method and the beach mark method. It is seen that the scatter of the aspect ratios for the individual surface cracks before the completion of coalescences is very large. These surface cracks can be replaced with a hypothetical single surface crack, (see Appendix). Figure 7 shows the result ($A \rightarrow B$) which is the change of aspect ratio of the representative single surface crack for the specimen width t_s of 7.5mm. It is understood that the aspect ratio decreases very rapidly as the crack advances because of the frequent coalescences. After the completion

of coalescences the aspect ratio increases as the crack advances ($B \rightarrow C \rightarrow D$).

Stress analyses are performed by using the three dimenional FEM. FEM mesh idealization used is shown in Fig.8. Calculation results are shown in Fig.9 and Fig.10.

Figure 11 (1) shows an approximate method of obtaining the stress intensity factor for a surface crack subjected to the uniform stress distribution along the crack line with the stress varying in the thickness direction. The results obtained in this particular case [6] are similar to those from the influence function method [10]. In the case that stress distribution shows the gradient over the width direction, the correction factor f in Fig.11 (2) is used in order to consider this effect on the stress intensity factor. ΔK at the deepest point of the surface crack in an early stage and of the through thickness crack after the penetration is obtained for the change of aspect ratio shown by the dotted thick curve in Fig.7.

The result is shown in Fig.12 in which abscissa X is defined as shown in Fig.13. When a surface crack is deeper than 0.8 times as large as the plate thickness, the K value has not been obtained yet because a correction factor for the front surface becomes very large. The changes of the stress intensity factor under the different loading conditions are established as shown in Fig.12. These calculation results are overlapping because of very small induced bending moment due to eccentricity by the exisitence of the gusset. Point C in Fig.12 corresponds to the K value for the surface crack, depth (a) of which is equal to $0.8W$ (W: plate thickness). Point D in the figure corresponds to the K value for a through thickness crack length $2c_0$.

Figure 14 shows the welding residual stress distributions in the cross section

of the plate at the boxing fillet weld toe, obtained using the inherent stress method [11]. The K value due to the welding residual stress is obtained based on using Fig.7 and Fig.14, and by adopting the K approximation method described above. The result is shown in Fig.15. Equivalent distributed stresses acting on a straight through thickness crack in an infinitely wide plate are introduced which reproduce the change of K with X for the advancing surface crack due to the applied loading and the welding residual stress. The corresponding variations of the equivalent stress with X are shown in Fig.16 and Fig.17 respectively. These relations and material constants are input to FLARP and then the RPG loads are calculated. An example of the simulation result on the RPG load is shown in Fig.18. The oscillation of the RPG load in Fig.18 derives from the discretization of the bar elements in the simulation. The oscillation can be reduced by applying the fine discretization of the bar elements.

A fatigue crack growth curve for a sound stress concentration part (i.e. without an initial crack) can be predicted subsequently, as exemplified by Fig.19. It is considered that slope of the crack growth curve decreases as the crack penetrates the zone of compressive residual stresses. The crack growth curve in Fig.19 based on ΔK_{RPG} is smooth even though RPG load history shows the oscillation in this calculation. Then, the oscillation of RPG load in Fig.18 can be ignored.

Figure 20 shows a simulated S-N curve in which the lives corresponding to the full thickness penetration are also shown. Estimated lives until the crack depth reaches first grain boundary and 1mm from the plate surface are also plotted. It is evident that the estimated penetration lives are in a very good agreement with the experimental ones. These results confirm that we can

assess crack initiation and growth curve from a sound stress concentration site of steel structures under in-service conditions in the design stage although it is currently time consuming to obtain the stress distributions from finite element analyses.

4 Concluding Remarks

A calculation algorithm for a fatigue crack growth curve from a sound stress concentration site for welded steel structures is established and a fatigue crack growth simulation code "FLARP" is developed. The ΔK_{RPG} or equivalent ΔK_{RPG} is used in the algorithm as the crack driving force parameter. This parameter represents the overlapping size of the tensile plastic zone at P_{max} and the compressive plastic zone at P_{min} in one loading cycle. FLARP is capable of evaluating effects of the stress ratio, overload, residual stress, grain size of steel, variable amplitude loading and sequence of load on fatigue initiation and growth curve [12][13]. Although this is not confirmed experimentally, we believe that FLARP can handle numerically the coaxing effect and the acceleration effects due to corrosion on fatigue crack growth.

Based on the experimental work, the procedure to account for changes of the aspect ratio for a surface crack in an arbitrary stress field is proposed to simulate the fatigue crack growth from a sound stress concentration site.

Although the crack growth predictions are made using the numerical code, preparing the input data, and specifically the stress distribution along the crack line by FEM, is currently extremely time-cosuming. Therefore, the required future work is to develop the suitable pre and post processors links

between FEM and FLARP.

Acknowledgements

This paper owes much to the thoughtful and helpful comments of Professor Malgorzata Skorupa, Faculty of Mechanical Engineering and Robotics, University of Mining and Metallurgy, Poland.

A Representative surface crack replacing plural surface cracks generated at the sound stress concentration site

It is observed that fatigue cracks usually initiate as plural surface cracks at a stress concentration site such as a fillet weld toe. These cracks coalesce as they advance, and finally a single large surface crack appears. It is also observed that the depth of the fatigue surface crack just after the completion of the coalescences is usually very small such as 0.5mm or so. Therefore the interference effects of neighboring surface cracks on the K value are studied for a semi-infinitely thick plate subjected to uniform tension. Following K values are used in Handbook [14].

Figure A-1 shows ratio of the K value at the deepest point of a semi-elliptical surface crack in the case of existing another surface crack of the same size to that of a single surface crack of the same size. Figure A-2 shows the decreasing ratio of the K value at the deepest point of a larger semi-circular surface crack in the presence of a smaller neighboring semi-circular surface crack to the K value when both cracks are of the same size. In that case the ratio of the K values for the abscissa of zero corresponds to a single semi-circular crack.

The ratio of the K values plotted against the distance between the two semi-circular cracks of the same size is shown in Fig.A-3. Figure A-4 is an alternative way of the presentation of the data from Fig.A-2 and demonstrates the interaction between two adjacent cracks. From the result that the K value is proportional to the square root of the crack area and from Fig.A-4, the method of a representative single surface crack, the depth of which is that of the deepest crack and the K value at the deepest point is the same as that for the deepest crack including the proximity effects, is developed, as shown in Fig.A-5. The representative crack method is illustrated in Fig.A-5 which shows that in the first stage the cracks (1) and (2) are replaced with crack (1'). Then in the next stage cracks (1') and (3) will be replaced by a single crack. It has been found that the order in which the replacements are done does not influence significantly the final result.

References

[1] Toyosada M. and Niwa T. Simulation Model of Fatigue Crack Opening/Closing Phenomena for Predicting RPG Load under Arbitrary Stress Distribution Field. Proceedings of the fifth International Offshore and Polar Engineering Conference,1995, 169–176.

[2] Satoh K., Toyoda M. Itoh Y. Kawaguchi Y. Arimochi K. Suzuki M. and Tatara T. Fracture Transition Behaviors and Fracture Overall Strain of Low Carbon Steel Plate with Notch. Journal of Society of Naval Architects of Japan 1977:142:148–155. (in Japanese)

[3] Toyosada M. and Niwa T. Prediction of fatigue life for steel structures. Kyouritsu publication, Tokyo, 2001. (in Japanese)

[4] Forsyth PJE. Fatigue Damage and Crack Growth in Alumium Alloys. Acta Metallurgica, 1963, 11:703–715.

[5] Gudjact HJ., Lendvai J., Schneider J., Wunderlich W. and Gerold V. Planar Slip and Deformation Induced Particle Dissolution in Cyclically Deformed Al-Li Single Crystal. Proceedings of fifth International Al-Li Conference, 1989, 1105–1114.

[6] Toyosada M., Niwa T. and Matsuda H. Growth Process and Assessment of Fatigue Life for Surface Cracks Emanated from Stress Concentration Field. Journal of Society of Naval Architects of Japan, 2001, 190:517–530. (in Japanese)

[7] Bilby BA., Cottrell AH. and Swinden KH. The Spread of Plastic Yield from a Notch. Proceedings of Royal Society of London, 1963, A:272:304–314.

[8] Hobson PD., Brown MW. and de los Rios ER. The Behavior of Short Fatigue Cracks. In Miller KJ. and de los Rios E. R., editors. EGF (ESIS) Publish, Mechanical Engineering Publication, London, 1986, 1:441–459.

[9] Navarro A. and de los Rios ER. A microstructurally short fatigue crack growth equation. Fatigue and Fracture of Engineering Materials and Structures, 1988, 11(5):383–396.

[10] Shiratori M., Miyoshi T. and Tanigawa K. Analysis of Stress Intensity Factors for Surface Cracks Subjected to Arbitrarily Distributed Surface Stresses. Journal of Mechanical Engineering of Japan, 1986, A:52(474):390–398. (in Japanese)

[11] Matsuoka K. and Yoshii T. Weld Residual Stress in Corner Boxing Joints. Class NK TECHNICAL BULLETIN, 1998, 16:1–10

[12] Toyosada M., Gotoh K. and Niwa T. Fatigue Crack Propagation for a Through Thickness Crack. International Journal of Fatigue, (now on contributing).

[13] Niwa T. and Toyosada M. A Study on Plastic Shrinkage Coefficient of Crack Opening/Closing model at a Crack Extension. Journal of Society of Naval Architects of Japan, 2000, 188:669–678.(in Japanese).

[14] Murakami Y., Hanson M.T., Hasebe N., Itoh Y., Kishimoto K., Miyata H., Miyazaki N., Terada H., Tohgo K. and Yuuki R., Stress Inensity factor Handbook. The Society of Materials Science Japan and Pergamon Press, 1992

Figure 1 Schematic dislocation density distribution along slip lines at a notch under unloading process in cyclic loading for a polycrystalline material

Figure 2 Size of the cyclic plastic region ahead of a shear crack in the first grain

Figure 3 Cohesive force model for a closed shear crack

Figure 4 Flow of calculation of fatigue crack growth curve from a sound stress concentration part by FLARP

Figure 5 Gusset type fatigue test specimen

Figure 6 Aspect ratio for each surface crack emanated at the toe of a boxing fillet weld before the completion of coalescences

Figure 7 Experimental result of the change of a hypothetical surface crack before the completion of coalescences and a surface crack after the completion

Figure 8 FEM model using solid elements for the gusset joint

Figure 9 Stress amplitude distribution along the thickness direction at the toe of boxing fillet toe for one fatigue loading condition

Figure 10 In-plane stress and out-of-plane stress distribution in the cross section at the fillet toe and Erdogan's equivalent membrane stress distribution for one fatigue loading condition (maximum load = 147 kN, minimum load = 7.4kN)

Figure 11 Approximate method to estimate the stress intensity factor at the deepest point of a surface crack in an arbitrary stress distribution field

Figure 12 Change of the stress intensity factor range as a crack advances from the boxing fillet weld toe for unit loading amplitude

Figure 13 Definition of reference crack length X

Figure 14 Analytical result on the residual stress distribution at the boxing fillet weld toe obtained using the inherent stress methodology

Figure 15 Change of stress intensity factor due to residual stress as a crack

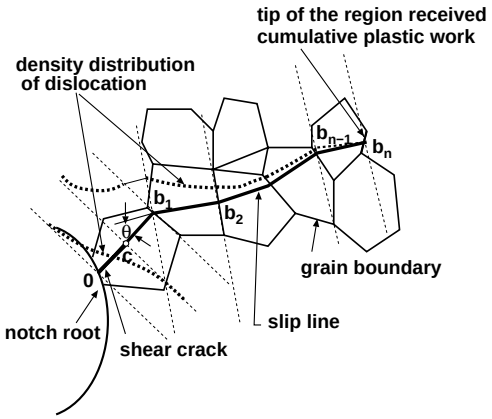

Figure 1

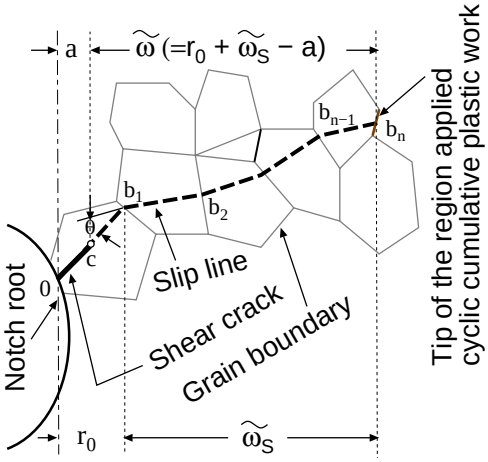

Figure 2

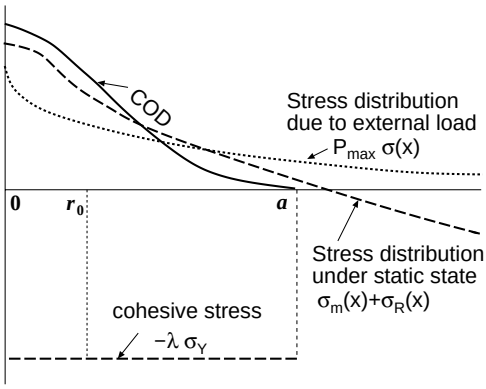

Figure 3

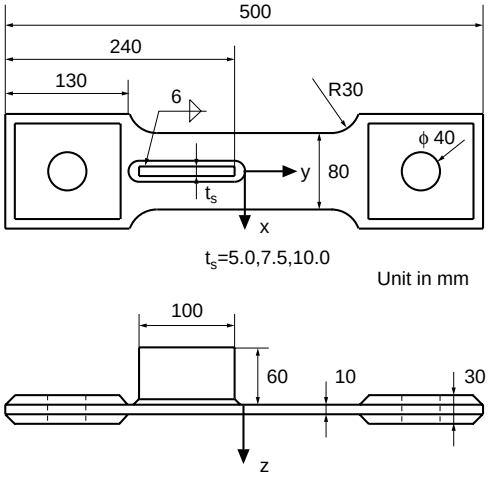

Figure 5

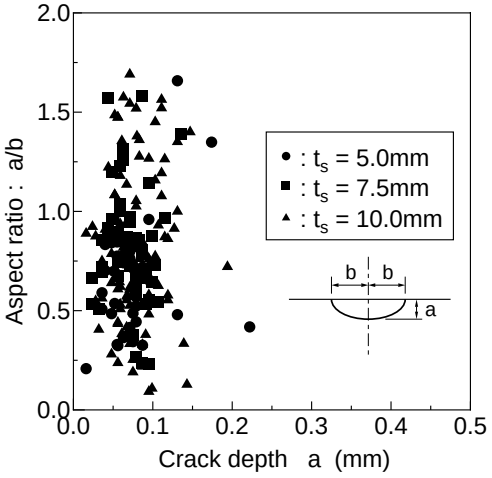

Figure 6

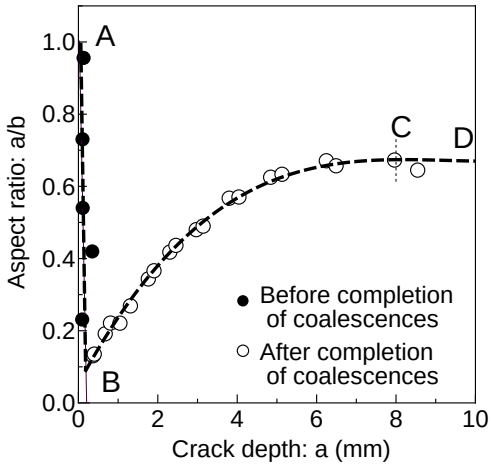

Figure 7

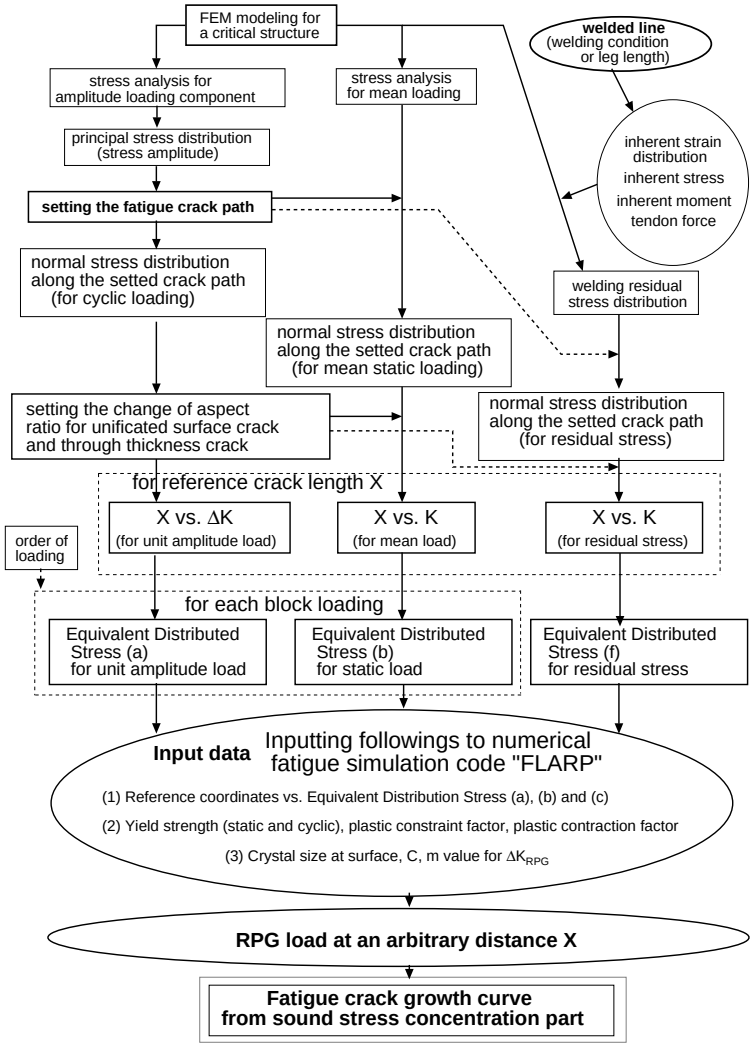

Figure 4

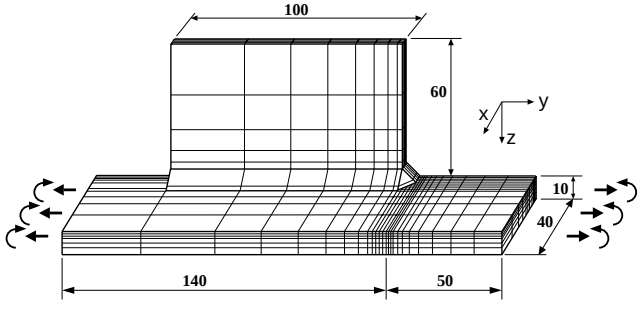

Figure 8

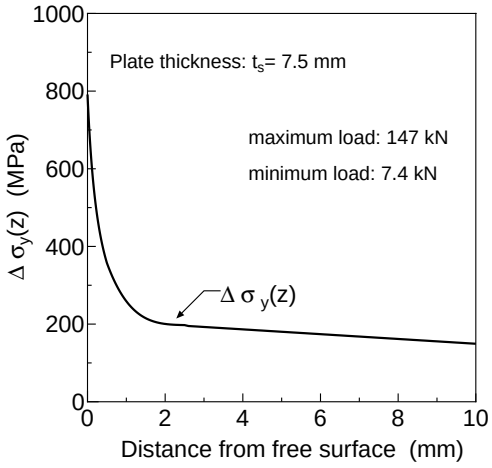

Figure 9

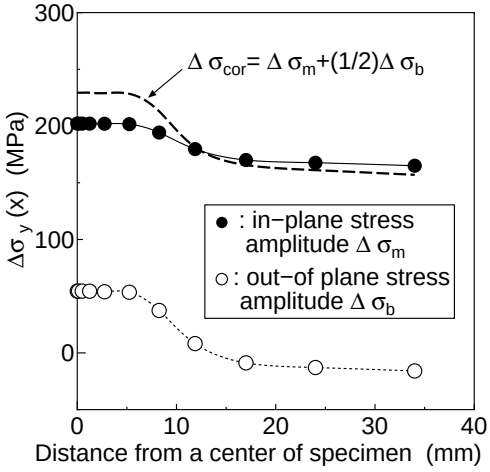

Figure 10

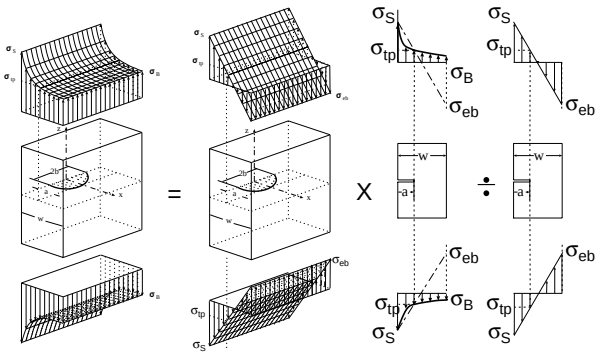

$K_{(a)}$ $K_{(b)}$ $K_{(c)}$ $K_{(d)}$

$$K_{(a)} = K_{(b)} K_{(c)} / K_{(d)}$$

(1) in case of uniform stress distribution along a crack line

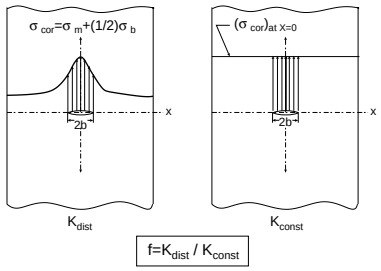

(2) Correction factor for stress distribution of equivalent tensile stress.

Stress intensity factor at the deepest point of a surface crack at the toe

of boxing fillet weld toe $= fK_{(a)}$

Figure 11

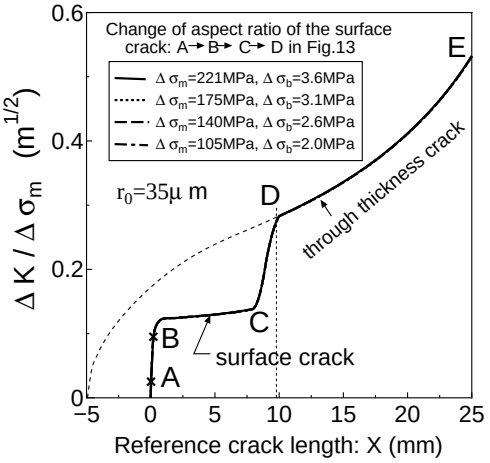

Figure 12

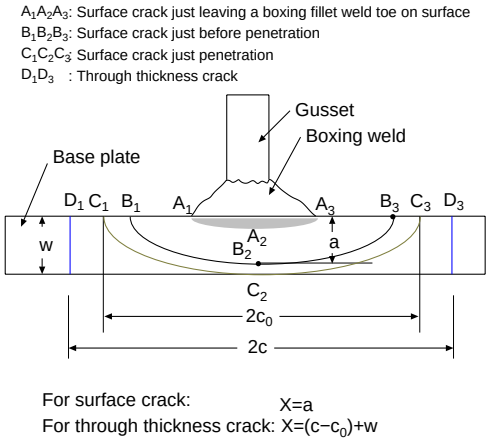

Figure 13

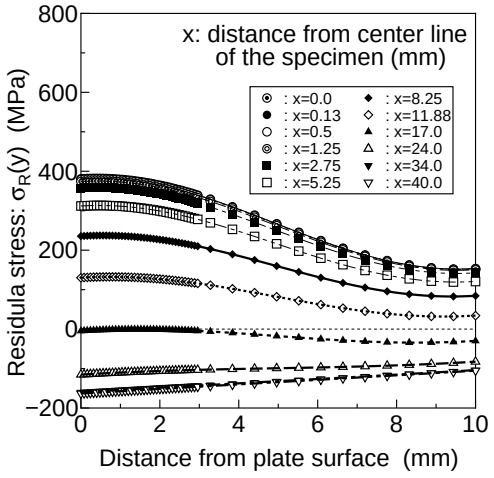

(a) Stress distribution in the plate at the center of the fillet weld toe

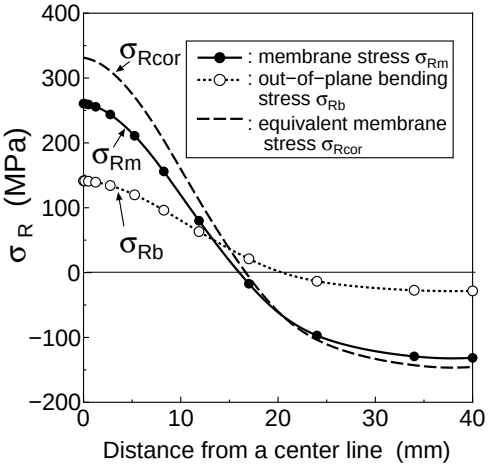

(b) Stress distribution of the membrane and bending stress

Figure 14

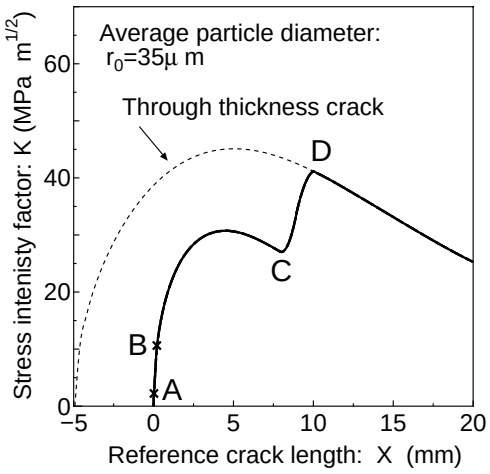

Figure 15

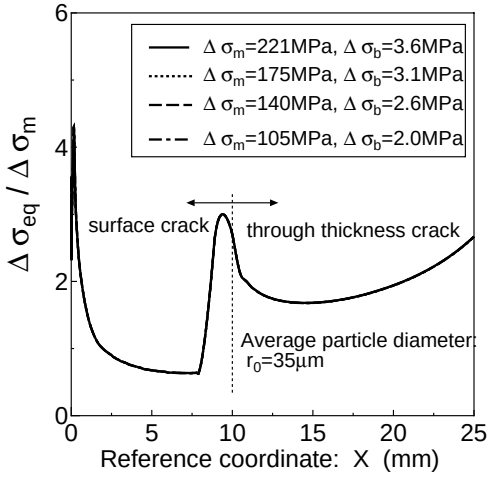

Figure 16

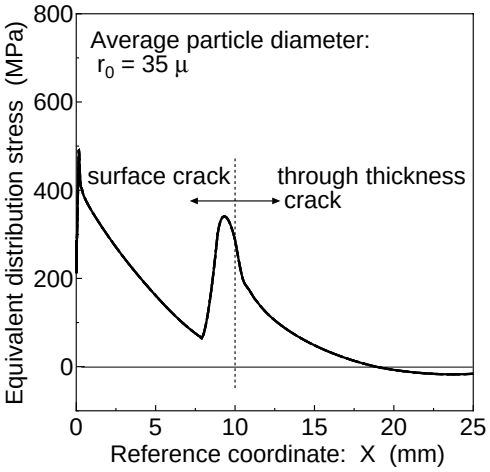

Figure 17

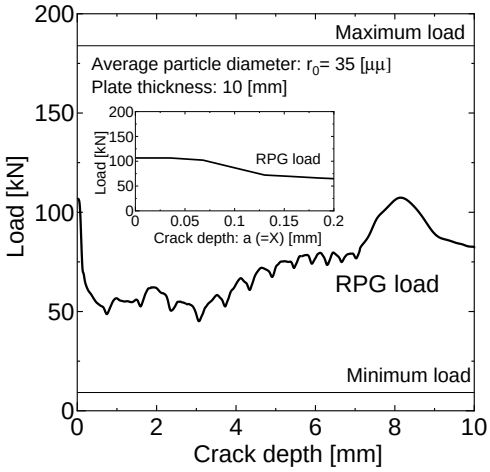

Figure 18

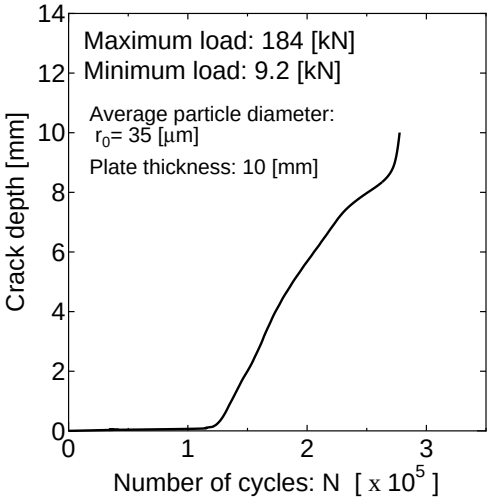

Figure 19

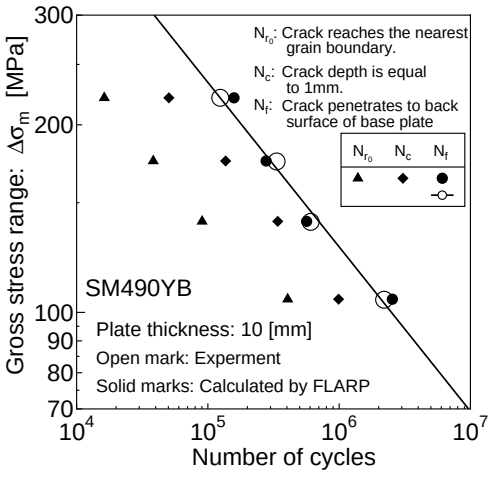

Figure 20

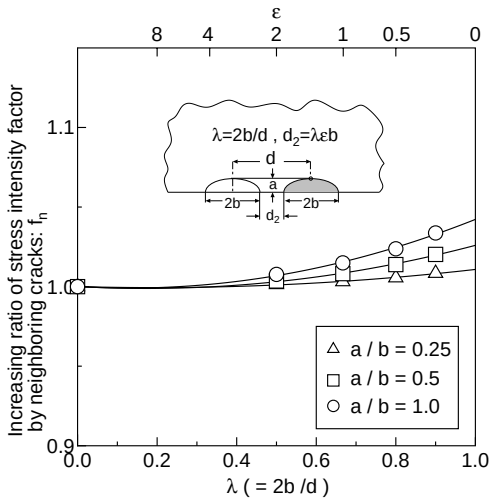

Figure A-1

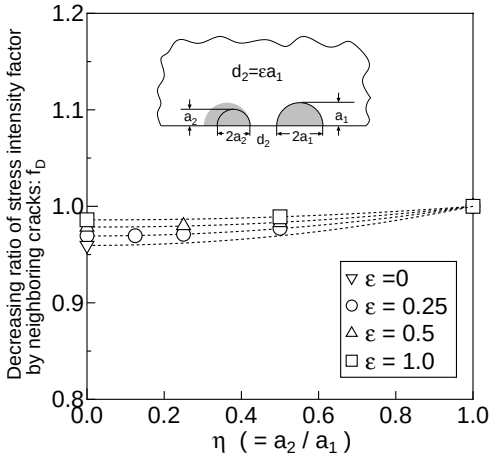

Figure A-2

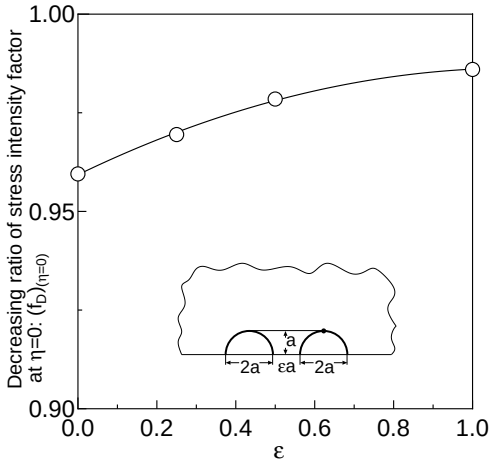

Figure A-3

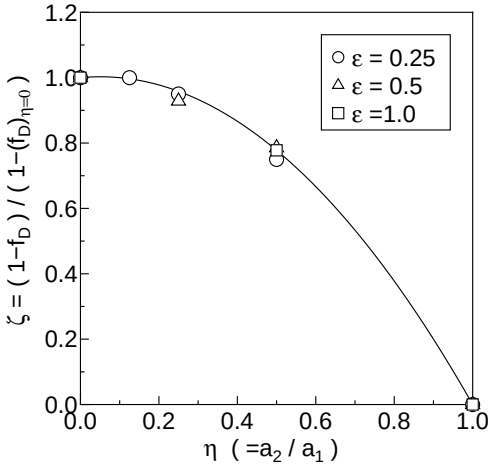

Figure A-4

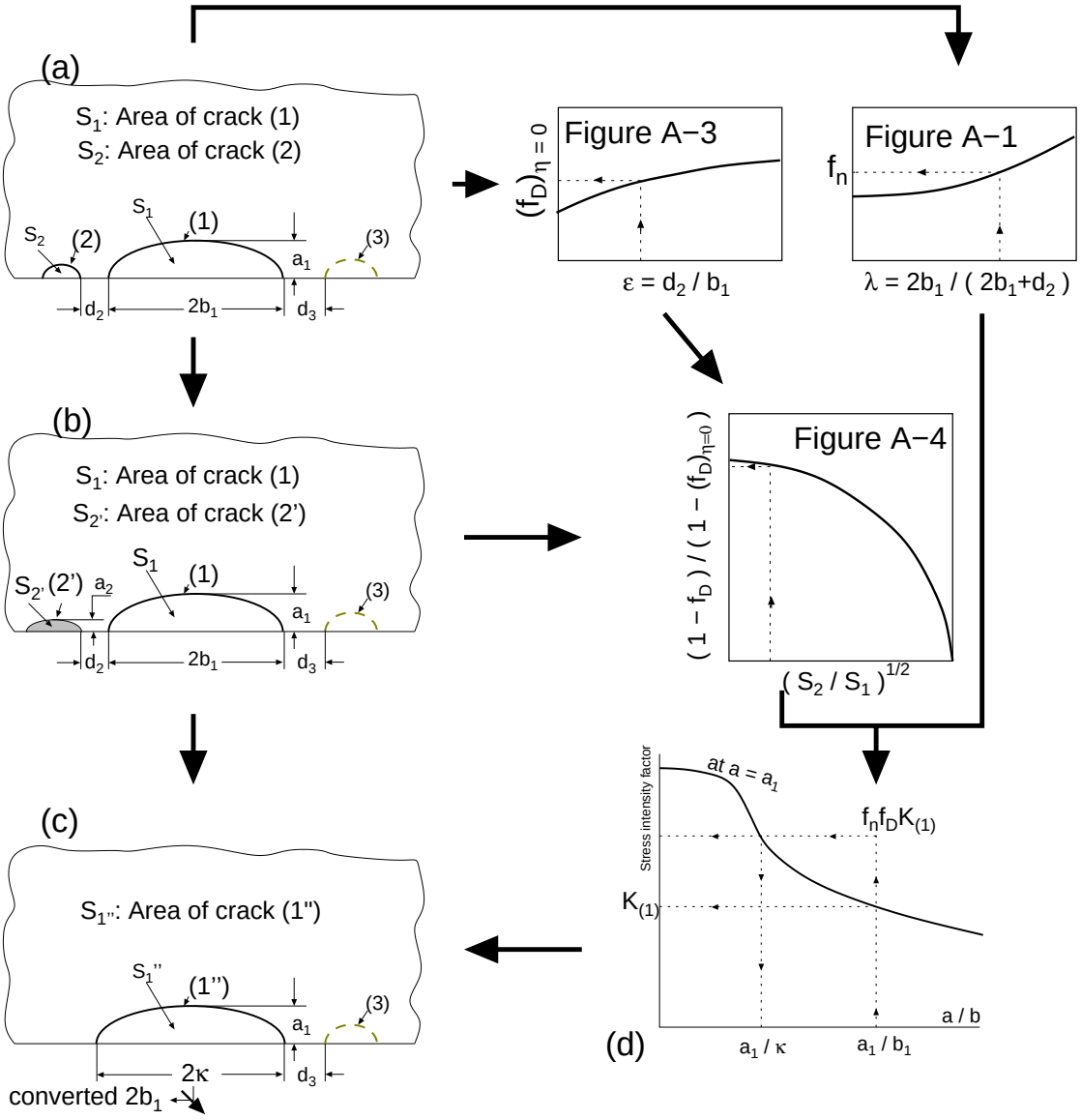
(a)
S1: Area of crack (1)
S2: Area of crack (2)
S1
(1)
S2
(2)
(3)
a1
d2
2b1
d3
(b)
S1: Area of crack (1)
S2': Area of crack (2')
S1
(1)
S2'
(2')
a2
(3)
a1
d2
2b1
d3
(c)
S1'': Area of crack (1")
S1''
(1'')
(3)
a1
2κ
d3
converted 2b1
Figure A−3
(fD)η = 0
ε = d2 / b1
Figure A−1
fn
λ = 2b1 / (2b1+d2)
Figure A−4
(1 − fD) / (1 − (fD)η=0)
(S2 / S1)1/2
(d)
Stress intensity factor
at a = a1
fnfDK(1)
K(1)
a / b
a1 / κ
a1 / b1

Figure A-5